

# Collective conical intersections through light-matter coupling in a cavity

Oriol Vendrell<sup>1, \*</sup>

<sup>1</sup>*Department of Physics and Astronomy, Aarhus University, Ny Munkegade 120, 8000 Aarhus C, Denmark<sup>†</sup>*

(Dated: August 13, 2018)

The ultrafast non-radiative relaxation of a molecular ensemble coupled to a cavity mode is considered theoretically and by real-time quantum dynamics. For equal coupling strength of single molecules to the cavity mode, the non-radiative relaxation rate from the upper to the lower polariton states is found to strongly depend on the number of coupled molecules. For  $N > 2$  molecules, the  $N - 1$  dark light-matter states between the two optically active polaritons feature true collective conical intersection crossings, whose location depends on the internal atomic coordinates of each molecule in the ensemble, and which contribute to the ultrafast non-radiative decay from the upper polariton. At least  $N = 3$  coupled molecules are necessary for cavity-induced collective conical intersections to exist and, for identical molecules, they constitute a special case of the Jahn-Teller effect.

The interaction of atoms and molecules with quantized light has the potential to open new routes towards manipulating their physical and chemical properties, and towards the development of hybrid matter-light systems with new attributes [1–6]. Over the past few years, ground breaking experiments that realize the aforementioned scenario using, e.g., microcavities, [7–11] have demonstrated the effective tuning of reaction rates and probabilities [9], energy transfer rates among different molecular species [12] and of molecular vibrations [13, 14]. A growing body of theoretical results [13, 15–29] has lead, among others, to propose mechanisms to suppress [20] and catalyze chemical processes [25] through a cavity mode, or modify the non-adiabatic dynamics of a single molecule strongly coupled to an electromagnetic mode [22].

Experimentally, it has been observed that photo-excitation of the upper polariton branch (UPB) in a coupled cavity-matter system is followed by population transfer to the lower polariton branch (LPB) before light emission from the UPB can take place [7, 10]. Time-resolved measurements in hybrid organic dye-molecule systems indicate that population transfer from the UPB to the LPB occurs within a time-scale of tens to hundreds of femtoseconds [10], orders of magnitude shorter than the radiative life-time of the molecular excited states in isolation. Theoretical predictions based on incoherent relaxation rates obtained by Fermi’s golden rule and based on modelling phonons coupled to the polaritonic excitation also predict relaxation rates of the order of tens to hundreds of femtoseconds [29, 30].

Even though it is well established that the ultrafast relaxation rates of molecular polaritons arise from vibronic interactions of the participant molecules [7, 29–31], a microscopic, real-time description of such phenomena, which additionally sheds light onto the connection with standard descriptions of non-radiative phenomena in chemical systems, is still missing. In this work, the vibronic interactions leading to ultrafast non-radiative decay of a molecular ensemble coupled a single electro-

magnetic mode will be discussed theoretically and on the basis of numerically converged quantum dynamics simulations. It will be shown how the vibronic origin of the ultrafast relaxation is of similar nature as for isolated molecular excitations and related to the existence of collective conical intersections (CCI) among dark states, whose topological properties will be discussed and compared to their intramolecular counterparts.

The starting point is an ensemble of non-interacting diatomic molecules aligned with the polarization axis of the quantized light mode (also referred throughout the paper as cavity mode). The Hamiltonian for this system reads

$$\hat{H} = \hat{T}_n + \hat{H}_{\text{el}} + \hat{H}_{\text{cav}} + \hat{H}_{\text{las}}, \quad (1)$$

where  $\hat{T} = \sum_{\kappa}^N \hat{t}_n^{(\kappa)}$  is the sum of nuclear kinetic energy operators for each  $\kappa$ -th molecule,  $\hat{H}_{\text{el}} = \sum_{\kappa}^N \hat{h}_{\text{el}}^{(\kappa)}$  is the sum of all other intramolecular Hamiltonian terms for each molecule

$$\hat{h}_{\text{el}}^{(\kappa)} = \hat{t}_e^{(\kappa)} + \hat{v}_{ee}^{(\kappa)} + \hat{v}_{en}^{(\kappa)} + \hat{v}_{nn}^{(\kappa)}, \quad (2)$$

$\hat{H}_{\text{cav}}$  is the cavity and cavity-ensemble Hamiltonian, and  $\hat{H}_{\text{las}}$  describes the eventual coupling to an external laser field. The terms in Eq. (2) correspond to the  $\kappa$ -th electronic kinetic energy and the Coulombic terms represent the electron-electron repulsion, electron-nuclei attraction and nuclei-nuclei repulsion, respectively. The cavity Hamiltonian is given by [17, 24, 28, 32]

$$\hat{H}_{\text{cav}} = \hbar\omega_c \left( \frac{1}{2} + \hat{a}^\dagger \hat{a} \right) + g \vec{\epsilon}_c \cdot \vec{D} (\hat{a}^\dagger + \hat{a}), \quad (3)$$

where  $\omega_c$  is the angular frequency of the cavity mode,  $\vec{\epsilon}_c$  is its polarization direction, and  $g = \sqrt{\hbar\omega_c/2V\epsilon_0}$  is the coupling strength between the cavity and the molecules where  $V$  is the quantization volume.  $\vec{D} = \sum_{\kappa}^N \vec{\mu}^{(\kappa)}$  is total dipole operator of the ensemble. In Eq. (3), the quadratic dipole self-energy term is being neglected, which is only relevant at much higher coupling strengths

than considered here. For further details see, e.g., Refs. [24, 32]. The coupling to an external laser field is introduced semiclassically in the length gauge and dipole approximation as  $\hat{H}_{\text{las}} = -\vec{E}(t)\vec{D}$ , where the electric field takes the form  $\vec{E}(t) = \epsilon_L A(t) \cos(\omega_L t)$ . It is assumed for simplicity that external laser fields couple to the molecules and do not pump the cavity mode directly. In general this is not necessarily the case and direct coupling to the cavity mode can be easily introduced [29]. However, since strong coupling is assumed (cf. discussion below), this model choice has only observable consequences at times below the Rabi cycling period of the hybrid system, in the order of a few tens of femtoseconds, and is not of relevance for our discussion.

As an illustrative molecular example we consider sodium iodide (NaI), whose ultrafast photo-dissociation dynamics in the first excited electronic state  $^1A$  coupled to the ground state  $^1X$  has been the subject of extensive experimental and theoretical investigations (See e.g., Ref. [33]), also in the context of cavity-induced chemistry [22, 28]. Details on the potential energy and transition dipole curves of NaI [28] and a detailed account of the quantum dynamics numerical techniques employed in this work can be found elsewhere [28, 34, 35]. Throughout this work the effective cavity-matter coupling is taken as  $g/\omega_c=0.01$ , where  $g$  was defined around Eq. (3) and can be seen as the rms vacuum electric field amplitude of the cavity mode [3]. This coupling strength is small compared to the single-molecule ultra-strong coupling regime, characterized by a Rabi splitting of the polaritonic energy levels (at zero detuning)  $\hbar\omega_R = 2g\mu_{01}$  comparable to the transition energy. The collective Rabi splitting is given by  $\hbar\Omega_R = 2g\mu_{01}\sqrt{N}$  [36], where  $N$  is the number of coupled molecules and  $\mu_{01}$  the transition dipole matrix element. For NaI at the Franck-Condon geometry this coupling strength results in  $\hbar\Omega_R = 0.13$  eV for  $N = 1$  and  $\hbar\Omega_R = 0.30$  eV for  $N = 5$ . Rabi splittings of this order have been observed experimentally in micro-cavities with coupled organic dye molecules [10, 12].

We note here that for an ensemble of molecules featuring a dissociative excited state and coupled to a cavity mode, photo-dissociation can only occur in the LPB. This is because, as one of the molecules dissociates, it ceases to be resonant with the cavity mode, the lower polariton turns into a pure electronic excitation of that molecule and the excitation energy is not available anymore for neither the cavity nor the other molecules, which subsequently remain in their respective ground states (cf. Fig. 1c). For this reason, the rate of photo-dissociation directly corresponds to the rate of relaxation from the UPB to the LPB, which will be used below.

We consider first the absorption spectra of a single isolated NaI molecule and compare it afterwards to the absorption spectra of a molecular ensemble. Excitation of an isolated NaI molecule to its first sin-

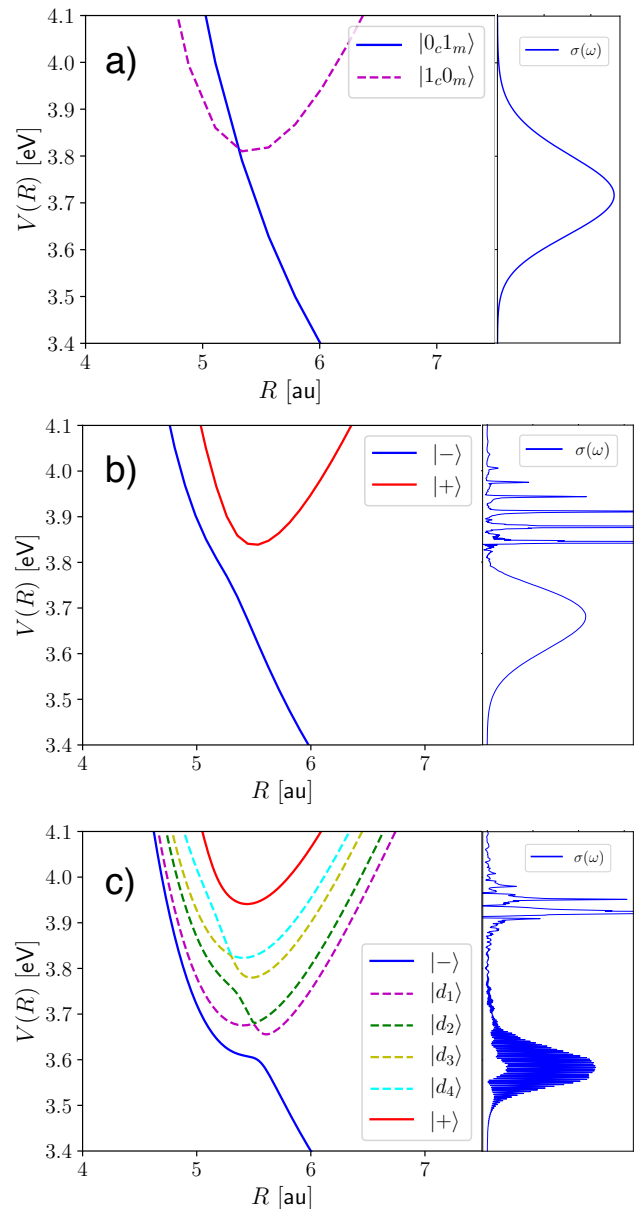


FIG. 1. Left panels: one-dimensional cuts along adiabatic polaritonic potential energy surfaces obtained by diagonalization of  $\mathcal{H}_{\text{el-cav}}^{[1]}(\mathbf{R})$  (cf. Eq. (4)). Right panels: absorption spectrum of the hybrid system (blue solid curves) and single-molecule photo-dissociation probability at the corresponding photon-energy (red dots). Isolated molecule (a), single coupled molecule (b) and ensemble of 5 molecules (c). Legends are explained in the main text.

glet excited electronic state results immediately in ballistic dissociation of the nuclear wave packet on the corresponding potential energy surface. Therefore, the photo-absorption spectrum features a single absorption band of, in this case, full width at half maximum (fwhm) about 0.2 eV centered at an excitation energy of about 3.7 eV, which is seen in the

right panel in Fig. (1a). The absorption spectrum  $\sigma(\omega) \propto \Re\{\omega \int_0^\infty e^{i\omega t} a(t) dt\}$  is computed from the dipole auto-correlation function  $a(t) = \langle \Psi_\mu(0) | e^{-i\hat{H}t/\hbar} | \Psi_\mu(0) \rangle$ , where  $|\Psi_\mu(0)\rangle = \vec{\epsilon}_L \cdot \vec{D} |\Psi_0\rangle$  and  $|\Psi_0\rangle$  is the ground state of the system. The strongly dissociative potential energy surface responsible for the fast dissociation is shown in the left panel of Fig. (1a), where the ground state potential energy surface shifted by the cavity photon energy  $V_0(R) + \frac{3}{2}\hbar\omega_c$  is shown as a dashed curve for comparison.

The photo-dissociation dynamics is significantly changed when the molecules are coupled to the cavity mode. In the case of a single molecule coupled to the cavity, the absorption spectrum is shown in the right panel of Fig. (1b). A broad absorption band is found in the energy region of the LPB and a set of discrete absorption peaks are seen in the region of the UPB. These markedly different spectral regions can be explained by the potential energy curves of the lower and upper polaritons obtained by diagonalization of the  $\hat{H}_{\text{el}} + \hat{H}_{\text{cav}}$  Hamiltonian as a function of  $R$ , which correspond to dissociative and bound potentials, respectively, and are shown in the left panel of Fig. (1b).

Population promoted to the LPB immediately dissociates as in the isolated molecule case. Conversely, the upper polariton features a sharp progression of long-lived vibrational excitations, which correspond, to a good approximation, to the vibrational energy levels on the ground electronic state potential energy surface shifted by the photon energy of the cavity mode. Clearly, there is no ballistic photo-dissociation from the upper polariton, as the LPB cannot be immediately reached.

The collective behaviour of a molecular ensemble is now investigated by increasing the number of molecules coupled to the cavity mode from  $N = 1$  to  $N = 5$  while keeping the same single-molecule coupling strength as before. The absorption spectrum is shown in the right panel in Fig. (1c). The LPB region features now a broad band with superimposed internal structure. The former is indicative of ballistic dissociation along one of the molecular coordinates, as in the single molecule case. The latter corresponds to bound-type dynamics along the other vibrational degrees of freedom [37, 38]. These dynamics of the LPB are observed independently of the number of molecules in the ensemble for  $N = 2$  up to  $N = 5$  (not shown) and will not be discussed further. In the UPB, the linear absorption spectrum still features several peaks reminiscent of the vibrational progression of the single molecule case, but broader, which is indicative of decay from those states within the first few hundreds of femtoseconds after photo-excitation.

The relaxation dynamics of the UPB in real time is accessed by pumping the system with an external laser of pulse of duration 30 fs (fwhm), photon energy tuned to the upper polariton region (cf. absorption spectra)

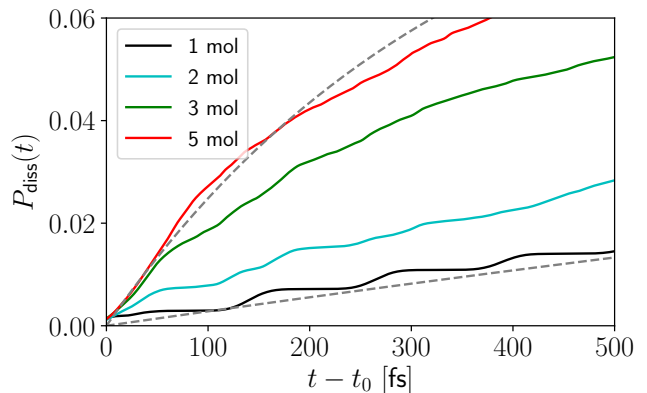


FIG. 2. Single-molecule photo-dissociation probability  $P_{\text{dis}}(t) = \langle \Psi(t) | \Theta(R_1 - R_b) | \Psi(t) \rangle$  as a function of time for an ensemble of different size interacting with a laser pulse of photon energy  $\hbar\omega_L = 3.9$  eV.  $R_b = 15$  au. The dashed curves correspond to fitted first order rate expressions.

and a peak field amplitude of  $5 \cdot 10^{-4}$  au. This relatively weak field ensures that in all cases light absorption takes place in the linear single photon regime. The time-dependent dissociation probability is defined as  $P_{\text{dis}}(t) = \langle \Psi(t) | \hat{\Theta}(R_1 - R_d) | \Psi(t) \rangle$ , where  $\Theta(x)$  is the Heaviside step function and  $R_d = 15$  au. As was mentioned above, the relaxation dynamics from the upper to the lower polariton branches can be traced through the probability of photo-dissociation, which can only occur in the LPB.

Inspection of  $P_{\text{dis}}(t)$  in Fig (2) for different ensemble sizes pumped to the UPB indicates that the dissociation occurs progressively, as compared to ballistic dynamics in the LPB. Even though the individual coupling of each molecule to the cavity, the laser parameters, and the total amount of population pumped by the laser to the UPB are the same in all cases, the rate of dissociation and therefore the rate of relaxation significantly depends on the size of the ensemble.

The calculated population curves in Fig (2) can be used to fit effective first order relaxation rate constants  $\kappa_N$  to the LPB starting from the UPB. For  $N = 5$ ,  $\kappa_5^{-1} \approx 350$  fs, whereas  $\kappa_1^{-1} \approx 3800$  fs. The first order rates result in the superimposed dashed curves in Fig. (2), which however do not completely capture all features of the quantum dynamics at short times. This marked dependence of the decay rate on the number of molecules is not found in expressions based on Fermi's golden rule and an assumed density of vibrational states [29, 30], and hints at the participation of decay pathways involving non-adiabatic nuclear dynamics with coupling between the electronic-polaritonic states and the vibrational degrees of freedom.

In order to shed light onto the nature of the relaxation pathways and to understand the origin of these different

kinds of dissociative dynamics, we direct our attention to the dark states found between the upper and lower polaritons. In the Tavis-Cummings model of an ensemble of two-level atoms coupled to a cavity, and in the zero-detuning case, all dark states are degenerate, appear at the average energy of the two bright polaritons and feature no dipole coupling to the ground state of the hybrid system [2]. Their dark nature is clearly manifest in Fig. (1c) by the practical lack of absorption between 3.65 and 3.85 eV in the linear absorption spectrum. When nuclear motion is present, the degeneracy of the dark states can be lifted through nuclear displacements that modulate the energy gap of the corresponding molecule. This leads to CCI among the dark polaritonic states, which are referred to as *collective* to emphasize the fact that their location in coordinate space depends on the internal coordinates of the different molecules in the ensemble. The existence of points of intersection among dark polaritonic states has been noted recently as well by Feist and collaborators [27].

A cut through the potential energy surfaces obtained by diagonalization of the  $\hat{H}_{\text{el}} + \hat{H}_{\text{cav}}$  Hamiltonian in the single-excitation space (SES) and for  $N = 5$  is shown in the left panel of Fig. (1c). For five molecules, six polaritonic states are present in the SES, two of which are the bright polaritons and four of them are nominally dark. In the cut shown,  $R_2 = R_3 = 5.35$  au,  $R_4 = R_5 = 5.5$  au, and  $R_1$  is scanned between 4 and 7.5 au. Two CCI, the origin of which will be discussed below, are seen along this PES cut at precisely  $R_1 = 5.35$  and  $R_1 = 5.5$ , which is not fortuitous.

The matrix representation of the  $\hat{H}_{\text{el}} + \hat{H}_{\text{cav}}$  operator in the basis of non-interacting cavity-ensemble states and in the SES results in the molecular Tavis-Cummings Hamiltonian [39]

$$\mathcal{H}_{\text{el-cav}}^{[1]} = \begin{pmatrix} \hbar\omega_c & \gamma^{(1)}(R_1) & \gamma^{(2)}(R_2) & \gamma^{(3)}(R_3) & \cdots \\ \gamma^{(1)}(R_1) & \Delta^{(1)}(R_1) & 0 & 0 & \cdots \\ \gamma^{(2)}(R_2) & 0 & \Delta^{(2)}(R_2) & 0 & \cdots \\ \gamma^{(3)}(R_3) & 0 & 0 & \Delta^{(3)}(R_3) & \cdots \\ \vdots & \vdots & \vdots & \vdots & \ddots \end{pmatrix}, \quad (4)$$

where  $\Delta^{(\kappa)}(R_\kappa) = V_1^{(\kappa)} - V_0^{(\kappa)}$  is the energy gap of the  $\kappa$ -th molecule and  $\gamma^{(\kappa)}(R_\kappa) = g\mu_{01}^{(\kappa)}$  is the dipole coupling of the  $\kappa$ -th molecule to the cavity mode. Hamiltonian (4) has the form of an arrowhead matrix, whose properties have been investigated in the contexts of applied mathematics [40, 41] and molecular physics [42].

The most important property of arrowhead matrices for our purposes is the fact that for every  $m$  molecules with the same energy gap  $\Delta$ , there is an eigenvalue  $\lambda_j = \Delta$  of multiplicity  $m - 1$  [41]. Hence, for  $m = 2$  molecules with the same energy gap, there is one eigenstate of  $\mathcal{H}_{\text{el-cav}}^{[1]}$  at the corresponding energy value. In

case  $m = 3$  molecules have the same energy gap, e.g., molecules 1 to 3, there are two degenerate eigenstates at that energy resulting in a CCI of order two. For the case of identical molecules, this degeneracy is found in the one-dimensional space  $R_1 = R_2 = R_3$  and it is lifted by displacements in the two-dimensional branching space that removes this equality. The local symmetry of the identical molecules giving rise to the CCI can be described in the permutation symmetry group  $S_3$  [43], which among others is isomorph with the  $D_3$  point group of an equilateral triangle [44]. As is well known, molecules of  $D_3$  and related symmetry point groups, e.g.  $C_{3v}$ , are Jahn-Teller active [44, 45] and the degeneracy of electronic state energies is lifted linearly for displacements out of the highly symmetric atomic arrangement, resulting in conically intersecting potential energy surfaces. Therefore, cavity-induced CCI are, from a mathematical standpoint, analogous to the commonly encountered [46] intra-molecular conical intersection case [44, 45, 47–49], including their divergent non-adiabatic coupling matrix elements  $\langle \psi_i | \vec{\nabla}_R | \psi_j \rangle$  at the regions of intersection [39], where  $|\psi_j\rangle$  are the eigenstates of  $\mathcal{H}_{\text{el-cav}}^{[1]}$ .

Generalising to larger numbers of molecules, the molecular Tavis-Cummings Hamiltonian features a CCI of order  $m - 1$  for any subset of  $m$  molecules at molecular geometries that result in an equal energy gap for all molecules of the subset. As a final example, the polaritonic states resulting of four identical molecules with the same geometry can be classified according to the symmetry representations of the  $S_4$  group, which is isomorph with the  $T_d$  point group of the tetrahedron and which leads to triply degenerate potential energy crossings and to the  $T_2 \otimes t_2$  Jahn-Teller effect [44].

Summarizing, real-time wave packet simulations of a molecular ensemble coupled to a cavity mode show that the non-radiative energy relaxation rate from the upper to the lower polaritonic states is strongly dependent on the number of coupled molecules. This is in contrast to descriptions based on Fermi's golden rule rates. Once the system reaches the manifold of nominally dark states, the vibronic relaxation dynamics proceeds through cavity-induced CCI, which mathematically are a consequence of the arrowhead-matrix form of the molecular Tavis-Cummings Hamiltonian in the SES. From a mechanistic perspective, the conical intersection topology funnels nuclear wave packets through it by first attracting them when in the upper part of the cone and then pushing them away once the probability amplitude appears on the lower electronic state [45]. This mechanistic idea represents the cornerstone of ultrafast non-radiative relaxation in isolated molecular systems. In the context of polariton relaxation, CCI may be an important ingredient for fast localization and decay of collectively coupled excitations. Since only the energy gap is determinant for the existence



of the CCI [41], these are expected to be robust against molecular rotations or other external perturbations that modulate the off-diagonal coupling strength of individual molecules to the cavity mode, as well as to local interactions with an environment, which will lead only to displacements of the locus of intersection. The precise role of CCI in collective decay mechanisms, specially for larger ensembles and more complex molecules, remains to be further investigated.

I want to thank L.B. Madsen, L.S. Cederbaum, H.-D. Meyer and J. Feist for insightful discussions.

---

\* e-mail: [oriol.vendrell@pci.uni-heidelberg.de](mailto:oriol.vendrell@pci.uni-heidelberg.de)

† Current affiliation: Theoretische Chemie, Physikalisch-Chemisches Institut, Universität Heidelberg, INF 229, 69120 Heidelberg, Germany

- [1] E. T. Jaynes and F. W. Cummings, *Proc. IEEE* **51**, 89 (1963).
- [2] M. Tavis and F. Cummings, *Phys. Lett. A* **25**, 714 (1967).
- [3] S. Haroche and D. Kleppner, *Phys. Today* **42**, 24 (1989).
- [4] R. Miller, T. E. Northup, K. M. Birnbaum, A. Boca, A. D. Boozer, and H. J. Kimble, *J. Phys. B: At Mol Opt Phys* **38**, S551 (2005).
- [5] H. Walther, B. T. H. Varcoe, B.-G. Englert, and T. Becker, *Rep. Prog. Phys.* **69**, 1325 (2006).
- [6] M. Aspelmeyer, T. J. Kippenberg, and F. Marquardt, *Rev. Mod. Phys.* **86**, 1391 (2014).
- [7] D. M. Coles, P. Michetti, C. Clark, W. C. Tsoi, A. M. Adawi, J.-S. Kim, and D. G. Lidzey, *Adv. Funct. Mater.* **21**, 3691 (2011).
- [8] T. Schwartz, J. A. Hutchison, C. Genet, and T. W. Ebbesen, *Phys. Rev. Lett.* **106**, 196405 (2011).
- [9] J. A. Hutchison, T. Schwartz, C. Genet, E. Devaux, and T. W. Ebbesen, *Angew. Chem. Int. Ed.* **124**, 1624 (2012).
- [10] T. Schwartz, J. A. Hutchison, J. Léonard, C. Genet, S. Haacke, and T. W. Ebbesen, *ChemPhysChem* **14**, 125 (2013).
- [11] T. W. Ebbesen, *Acc. Chem. Res.* **49**, 2403 (2016).
- [12] X. Zhong, T. Chervy, L. Zhang, A. Thomas, J. George, C. Genet, J. A. Hutchison, and T. W. Ebbesen, *Angew. Chem. Int. Ed.* **56**, 9034 (2017).
- [13] J. George, S. Wang, T. Chervy, A. Canaguier-Durand, G. Schaeffer, J.-M. Lehn, J. A. Hutchison, C. Genet, and T. W. Ebbesen, *Faraday Discuss.* **178**, 281 (2015).
- [14] J. George, T. Chervy, A. Shalabney, E. Devaux, H. Hiura, C. Genet, and T. W. Ebbesen, *Phys. Rev. Lett.* **117**, 153601 (2016).
- [15] G. Morigi, P. W. H. Pinkse, M. Kowalewski, and R. de Vivie-Riedle, *Phys. Rev. Lett.* **99**, 073001 (2007).
- [16] F. Caruso, S. K. Saikin, E. Solano, S. F. Huelga, A. Aspuru-Guzik, and M. B. Plenio, *Phys. Rev. B* **85**, 125424 (2012).
- [17] J. Galego, F. J. Garcia-Vidal, and J. Feist, *Phys. Rev. X* **5**, 041022 (2015).
- [18] J. Schachenmayer, C. Genes, E. Tignone, and G. Pupillo, *Phys. Rev. Lett.* **114**, 196403 (2015).
- [19] J. A. Ćwik, P. Kirton, S. De Liberato, and J. Keeling, *Phys. Rev. A* **93**, 033840 (2016).
- [20] J. Galego, F. J. Garcia-Vidal, and J. Feist, *Nat. Commun.* **7**, 13841 (2016).
- [21] F. Herrera and F. C. Spano, *Phys. Rev. Lett.* **116**, 238301 (2016).
- [22] M. Kowalewski, K. Bennett, and S. Mukamel, *J. Phys. Chem. Lett.* **7**, 2050 (2016).
- [23] M. Kowalewski, K. Bennett, and S. Mukamel, *J. Chem. Phys.* **144**, 054309 (2016).
- [24] J. Flick, M. Ruggenthaler, H. Appel, and A. Rubio, *Proc. Natl. Acad. Sci.* **114**, 3026 (2017).
- [25] J. Galego, F. J. Garcia-Vidal, and J. Feist, *Phys. Rev. Lett.* **119**, 136001 (2017).
- [26] H. L. Luk, J. Feist, J. J. Toppari, and G. Groenhof, *J. Chem. Theory Comput.* **13**, 4324 (2017).
- [27] J. Feist, J. Galego, and F. J. Garcia-Vidal, *ACS Photonics* **5**, 205 (2017).
- [28] O. Vendrell, *Chem. Phys.* **509**, 55 (2018).
- [29] R. Sáez-Blázquez, J. Feist, A. I. Fernández-Domínguez, and F. J. García-Vidal, *arXiv*, 1804.01784 (2018).
- [30] V. M. Agranovich, M. Litinskaia, and D. G. Lidzey, *Physical Review B* **67**, 085311 (2003).
- [31] R. F. Ribeiro, L. A. Martínez-Martínez, M. Du, J. Campos-Gonzalez-Angulo, and J. Yuen-Zhou, *Chem. Sci.* **9**, 6325 (2018).
- [32] F. H. M. Faisal, *Theory of Multiphoton Processes* (Springer US, 1987).
- [33] A. H. Zewail, *Science* **242**, 1645 (1988).
- [34] U. Manthe, H.-D. Meyer, and L. S. Cederbaum, *J. Chem. Phys.* **97**, 3199 (1992).
- [35] M. H. Beck, A. Jäckle, G. A. Worth, and H.-D. Meyer, *Phys. Rep.* **324**, 1 (2000).
- [36] R. J. Thompson, G. Rempe, and H. J. Kimble, *Phys. Rev. Lett.* **68**, 1132 (1992).
- [37] E. J. Heller, *Acc. Chem. Res.* **14**, 368 (1981).
- [38] D. J. Tannor, *Introduction to quantum mechanics: a time-dependent perspective*, edited by L. A. Young (University Science Books, 2007).
- [39] See supporting Information.
- [40] J. H. Wilkinson, *Oxford: Clarendon Press, 1965* (1965).
- [41] D. O’Leary and G. Stewart, *J. Comput. Phys.* **90**, 497 (1990).
- [42] O. Walter, L. S. Cederbaum, and J. Schirmer, *J. Math. Phys.* **25**, 729 (1984).
- [43] P. R. Bunker and P. Jensen, *Molecular Symmetry and Spectroscopy*, 2nd ed. (NRC Research Press, 1998) p. 747.
- [44] H. Köppel, D. R. Yarkony, and H. Barentzen, eds., *The Jahn-Teller Effect* (Springer Berlin Heidelberg, 2010).
- [45] W. Domcke, D. R. Yarkony, and H. Köppel, eds., *Conical Intersections: Electronic Structure, Dynamics & Spectroscopy* (World Scientific Pub Co. Inc., 2004).
- [46] D. Truhlar and C. Mead, *Phys. Rev. A* **68**, 032501 (2003).
- [47] D. R. Yarkony, *Rev. Mod. Phys.* **68**, 985 (1996).
- [48] D. R. Yarkony, *Acc. Chem. Res.* **31**, 511 (1998).
- [49] G. A. Worth and L. S. Cederbaum, *Annu. Rev. Phys. Chem.* **55**, 127 (2004).